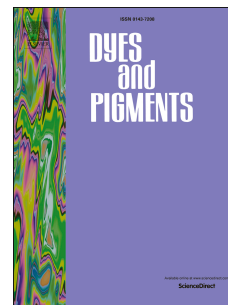


Journal Pre-proof

Ruthenium-based phosphorescent probe for selective and naked-eye detection of cyanide in aqueous media

Jing-Wei Zhu, Hui-Dan Ou, Niwei Xu, Wei Deng, Zi-Jian Yao



PII: S0143-7208(19)32565-3

DOI: <https://doi.org/10.1016/j.dyepig.2020.108196>

Reference: DYPI 108196

To appear in: *Dyes and Pigments*

Received Date: 6 December 2019

Revised Date: 8 January 2020

Accepted Date: 8 January 2020

Please cite this article as: Zhu J-W, Ou H-D, Xu N, Deng W, Yao Z-J, Ruthenium-based phosphorescent probe for selective and naked-eye detection of cyanide in aqueous media, *Dyes and Pigments* (2020), doi: <https://doi.org/10.1016/j.dyepig.2020.108196>.

This is a PDF file of an article that has undergone enhancements after acceptance, such as the addition of a cover page and metadata, and formatting for readability, but it is not yet the definitive version of record. This version will undergo additional copyediting, typesetting and review before it is published in its final form, but we are providing this version to give early visibility of the article. Please note that, during the production process, errors may be discovered which could affect the content, and all legal disclaimers that apply to the journal pertain.

© 2020 Published by Elsevier Ltd.

CRedit author statement

Jing-Wei Zhu: Ph.D student, Conceptualization, Methodology and Writing original draft;

Hui-Dan Ou: Ph.D student, Methodology and Characterization;

Ni-Wei Xu, Methodology, Characterization and Writing-Review and Editing;

Wei Deng, Co-supervision;

Zi-Jian Yao, Supervision, Conceptualization, Methodology, Writing-Review and Editing.

Journal Pre-proof

Ruthenium-based phosphorescent probe for selective and naked-eye detection of cyanide in aqueous media

Jing-Wei Zhu,^a Hui-Dan Ou,^a Niwei Xu,^c Wei Deng,^{*a} Zi-Jian Yao^{*a, b}

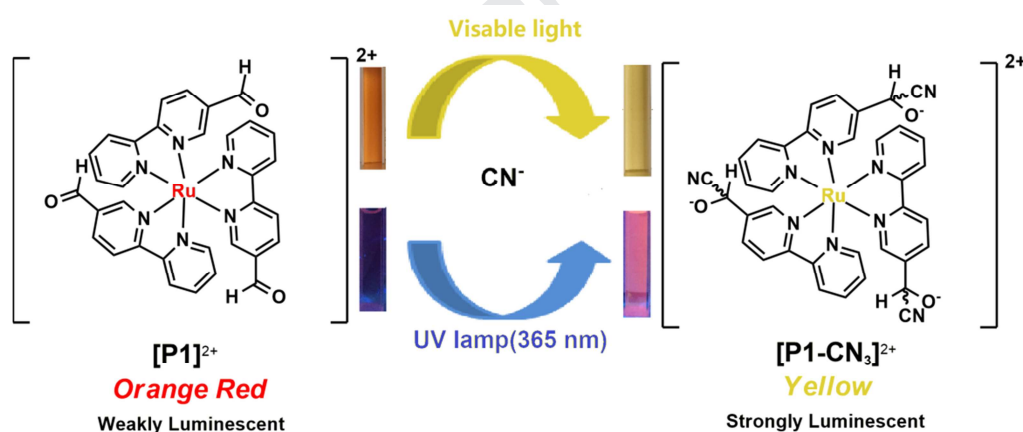
^a School of Chemical and Environmental Engineering, Shanghai Institute of Technology, Shanghai, 201418, China.

^b State Key Laboratory of Chemo/Biosensing and Chemometrics, Hunan University, Changsha 410082, China

^c Hunan Traditional Chinese Medical College, Zhuzhou, 412012, China

Corresponding author: Email: zjyao@sit.edu.cn; Tel: +86-21-60877231, Fax: +86-21-60873335.

(Graphical Abstract)



The ruthenium probe exhibits highly selective and sensitive for CN^- recognition in aqueous solution (60 % water) with a detection limit of 0.75 μM . Changes in the color of the solution were clearly observed with the naked eye. Based on the color change of the solution, a strip was prepared and showed good detection performance CN^- ion and quick response time.

Ruthenium-based phosphorescent probe for selective and naked-eye detection of cyanide in aqueous media

Jing-Wei Zhu,^a Hui-Dan Ou,^a Niwei Xu,^c Wei Deng,^{*a} Zi-Jian Yao^{*a, b}

^a School of Chemical and Environmental Engineering, Shanghai Institute of Technology, Shanghai, 201418, China.

^b State Key Laboratory of Chemo/Biosensing and Chemometrics, Hunan University, Changsha 410082, China

^c Hunan Traditional Chinese Medical College, Zhuzhou, 412012, China

Corresponding author: Email: zjyao@sit.edu.cn; Tel: +86-21-60877231, Fax: +86-21-60873335.

Abstract: A simple molecular phosphorescent Ru(II) probe **P1** has been synthesized by the reaction of 5-aldehyde-2,2'-bipyridine with ruthenium(II) chlorides under mild conditions. The probe upon interaction with different cation and anion showed high selectivity and sensitivity for cyanide ion (CN⁻) through phosphorescence “turn-on” response in aqueous solution (60 % water) with a detection limit of 0.75 μM. The significant phosphorescence enhancement (~ 30-fold) is attributed to the nucleophilic addition of cyanide ion to the aldehyde groups of the ruthenium complex in 3 : 1 stoichiometry, in which a naked-eye sensitive orange red color of solution changed to a yellow. The generation of cyanohydrin species through nucleophilic addition has been confirmed by ¹H NMR, FT-IR and mass spectra. Based on the color change of the solution, a visual colorimetric strip was prepared, which also showed good detection performance on cyanide ion with quick response time. The prominent efficiency of the Ru(II) probe proved the potential possibility of application in biosystems relating with cyanide ion.

Keywords: Ruthenium complex, cyanide, probe, aqueous media.

Introduction

Cyanide ion (CN^-) as an extremely toxic inorganic anion is harmful to the environment and human health.¹ However, its wide range of application, particularly in gold mining, electroplating, and various chemical industries, leads to unavoidable environmental spills [1, 2]. It is inevitable that some cyanide ion will leak into domestic water along with industrial waste-water. The maximum concentration of cyanide in drinking water published by the world health organization is $1.9 \mu\text{M}$ [3]. Due to the irreplaceability of cyanide in industrial production, it is necessary to use a simple and intuitive method to selectively detect the cyanide content. So far, various types of colorimetric and fluorescent receptors have been considered as excellent sensor materials for cyanide ions, and reactive fluorescent probes are becoming a hot research direction due to their advantages of selectivity, sensitivity, rapid and intuitive detection [4–6].

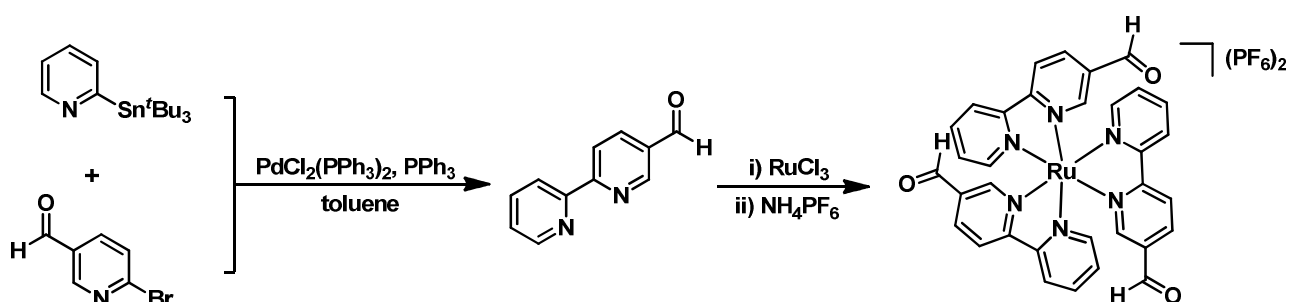
Ruthenium(II) polypyridyl complexes of 2,2'-bipyridine(bpy) [7–10] and related ligands [11–13] have interesting photophysical, photochemical, and electrochemical properties that make them attractive for development of luminescent sensors [14, 15], dye-sensitized solar cells [16–19], photoinduced switches [20–23], and photoactive devices [24–27]. The phosphorescent ruthenium(II) polypyridine complexes as chemosensors [28, 29] has recently attracted tremendous interest owing to their favorable photophysical properties, such as visible excitation wavelengths, large Stoke shifts, relatively long excited state lifetimes, suitable redox properties for electrochemiluminescence, and high stability in aqueous media compared with those of pure organic luminophores. Recently, a huge number of chromogenic and luminescent receptors / probes based on ruthenium(II) polypyridine complexes has been synthesized for the selective and sensitive sensing of metal cations [30, 31], anions [32–34], molecular oxygen [35–37], and biologically relevant molecules [38–40].

The cyanide has a strong affinity for electron-deficient carbonyl units capable of forming cyanohydrins, thus the interferences from acetate and fluoride can be minimized by designing a novel chemosensor particularly for cyanide [41–46]. Herein, we report the synthesis of a remarkable bipyridine based colorimetric probe **P1** (Scheme 1), and its application towards cyanide ion (CN^-) detection. The interaction of the designed ruthenium(II) complex with cyanide ion was researched by UV-vis absorption, photoluminescence (PL), FT-IR, and ^1H -NMR spectroscopy. The effect of water content in the solvent on phosphorescence, the expansion of the contrast ion species and the feasibility study as a colorimetric test paper also have been performed to prove whether the probe has the possibility of practical application.

Results and discussion

Synthesis of phosphorescent Ru(II) probe P1. The ligand 5-aldehyde-2,2'-bipyridine **L** was prepared by direct reactions from 2-(tributylstannyl)pyridine and 6-bromo-3-pyridinecarbaldehyde under N_2 atmosphere according to the reported procedures (Scheme 1) [47–49]. The color of the turbid liquid changes rapidly from yellow to black after reaching the set temperature. The ligand was obtained in high yields as white or light yellow solids. With the ligands in hand, the reactivity of **L1** with ruthenium trichloride was investigated in the presence of ethanol and water as the solution. The black-colored solution mixture gradually became clear red solution as the reaction went on. The target product tris (5-aldehyde-2,2'-bipyridyl) Ru (II) hexafluorophosphate was collected in an appropriate manner at room temperature as an air-stable dark red solid. The product is soluble in acetone, acetonitrile and DMSO, slightly soluble in CH_2Cl_2 , but insoluble in non-polar solvents such as diethyl ether and hexane. The Ligand acts as a chelate through the *N*, *N*-coordination mode of the product which is supported by FT-IR and ^1H NMR spectroscopy. **P1**

was fully characterized by various spectroscopic techniques.



Scheme 1. Synthesis of **P1**. For a detailed synthetic procedure, see the Experimental section.

Crystal Structure of P1. To unambiguously elucidate the molecular structure of the **P1**, we dissolved the **P1** in acetonitrile, and then slowly diffused into the ether solution to obtain a single crystal suitable for the **P1** suitable for single crystal diffraction analysis. Compounds **P1** were found to crystallize in the triclinic space group $P\bar{1}$. Its single crystal structure is shown in Fig. 1. Selected geometric data are given in supporting information. The structures revealed that the ruthenium centers adopt a similar octahedral geometry through tridentate coordination of three bipyridines ligand (Fig. 1). The distances of Ru–N bonds in the complex are 2.1(4) Å (Ru–N(1)), 2.1(4) Å (Ru–N(2)), 2.0(4) Å (Ru–N(3)), 2.1(4) Å (Ru–N(4)), 2.1(4) Å (Ru–N(5)) and 2.1(5) Å (Ru–N(6)) are within the range of known values for the bond in similar ruthenium complexes [50]. The bond lengths of C(11)–O(1), C(22)–O(2) and C(33)–O(3) are 1.2(8) Å, 1.2(9) Å, and 1.2(12) Å, respectively, which are also consistent with previous reports [66]. The angles of N–Ru–N are 78.9(17)° (N(1)–Ru–N(2)), 78.7(19)° (N(3)–Ru–N(4)), 78.2(2)° (N(6)–Ru–N(5)). The dihedral angle between different bipyridines has been calculated are 84.8° (N(2)–C(1)–N(1) and N(4)–C(12)–N(3)), 80.5° (N(4)–C(12)–N(3) and N(6)–C(23)–N(5)) and 85.8° (N(2)–C(1)–N(1) and N(6)–C(23)–N(5)).

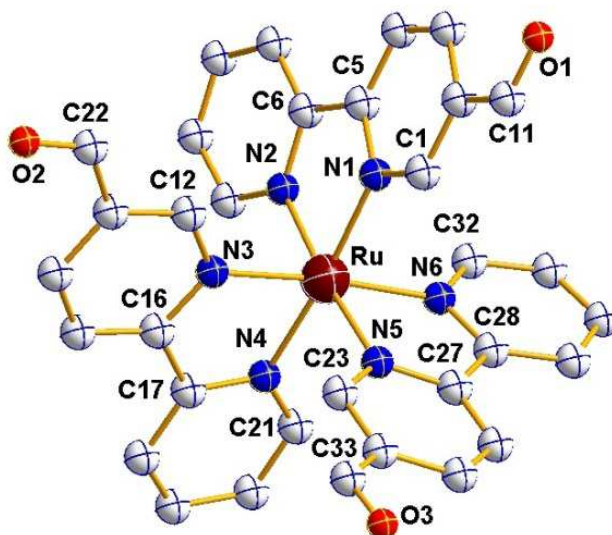


Fig. 1. Molecule structure of the ruthenium compound **P1** (thermal ellipsoids were drawn at the 30% probability level). All hydrogen atoms are omitted for clarity. Selected bond lengths (Å) and angles (deg): Ru–N(1), 2.057(4); Ru–N(2), 2.065(4); Ru–N(3), 2.045(4); Ru–N(4), 2.059(4); Ru–N(5), 2.063(4); Ru–N(6), 2.062(5); N(1)–C(1), 1.338(7); N(2)–C(6), 1.361(7); N(3)–C(16), 1.355(7); N(4)–C(17), 1.330(8); N(5)–C(23), 1.333(9); O(1)–C(11), 1.202(9); O(2)–C(22), 1.206(8); C(33)–O(3), 1.229(12); N(6)–C(28), 1.375(8); N(1)–Ru–N(2), 78.94(17); N(3)–Ru–N(4), 78.77(19); N(6)–Ru–N(5), 78.2(2); C(1)–N(1)–C(5), 118.7(5); C(12)–N(3)–C(16), 118.6(5); C(23)–N(5)–C(27), 119.3(6).

UV–vis spectrum analysis of P1. UV–vis spectrum of **P1** in CH₃CN displays sharp bands at approximately 300 nm assigned to intraligand (IL) π – π^* transitions. Additionally, the broad metal–to–ligand charge–transfer (MLCT) absorption is observed in the 425–550 nm range consisting of two or more MLCT bands (Fig. 2a) [51–54]. The ability of the newly developed **P1** to act as a chemosensor for different anions (3.0 equiv.) has been examined by UV-vis absorption and photoluminescence spectroscopy in CH₃CN solution at room temperature. The UV-vis spectrum of **P1** display significant absorption changes exclusively in the presence of CN[–] (Fig. 2). Upon addition of 3.0 equiv. of CN[–] to an acetonitrile solution of **P1** and the absorption maximum dramatically blue shifted from 475 to 375 nm ($\Delta\lambda = 30$ nm). A prominent orange to yellow color

change was observed (inset of Fig. 2b). In contrast, no significant changes of λ_{\max} and the color were observed in the presence of other anions, such as AcO^- , Br^- , Cl^- , ClO_4^- , CN^- , CO_3^{2-} , PO_4^{3-} , SO_4^{2-} , OH^- , Et-S^- , Ph-S^- , Ph-NH_2 , Ca^{2+} , Na^+ , CN^- , K^+ , NH_4^+ , F^- and Zn^{2+} (Fig.3). The reaction of an aldehyde group attached to the 5-position of the N-coordinating pyridyl moiety of the ligand with CN^- is selective through the above observations. UV-vis titration experiments have been implemented to understand more about the reasons for the color change. The incremental addition of CN^- (0.0–3.0 equiv.) to the CH_3CN solution of **P1** (20 μM) at room temperature reveals a gradual decrease of LLCT peak at 310 nm and the absorption maximum gradually blue shifted from 450–500 nm to 420–470 nm ($\Delta\lambda = 30$ nm) (Fig.2) [55]. The different colors before and after addition of CN^- ions could be easily distinguished by the naked eye (inset of Fig. 2b).

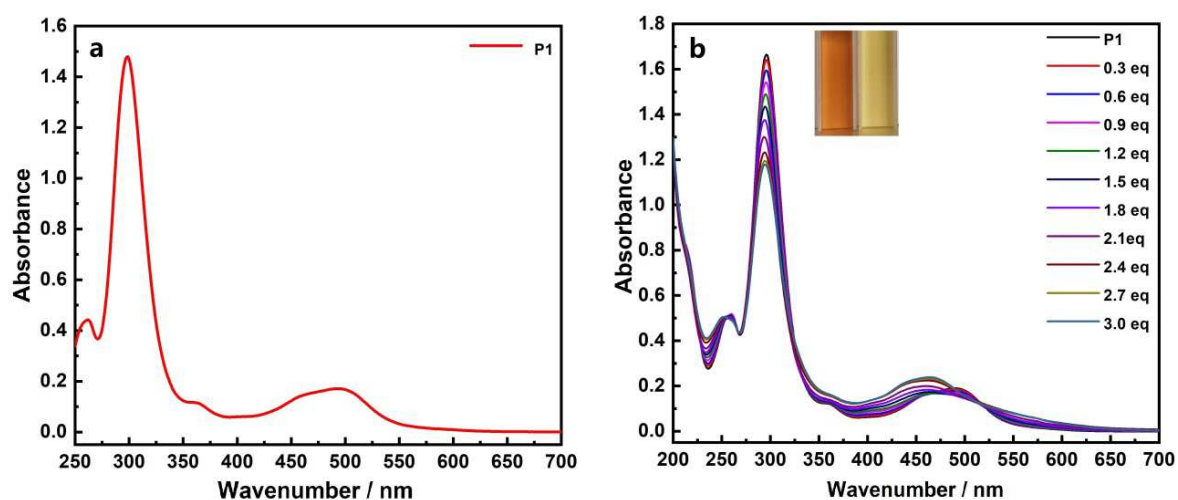


Fig. 2. (a) UV-vis spectrum of **P1** (20 μM); (b) **P1** solution is added to the equivalent of CN^- (0.3 eq / time) UV titration image (inset: left: **P1**, right: **P1** + 3.0 eq. CN^-).

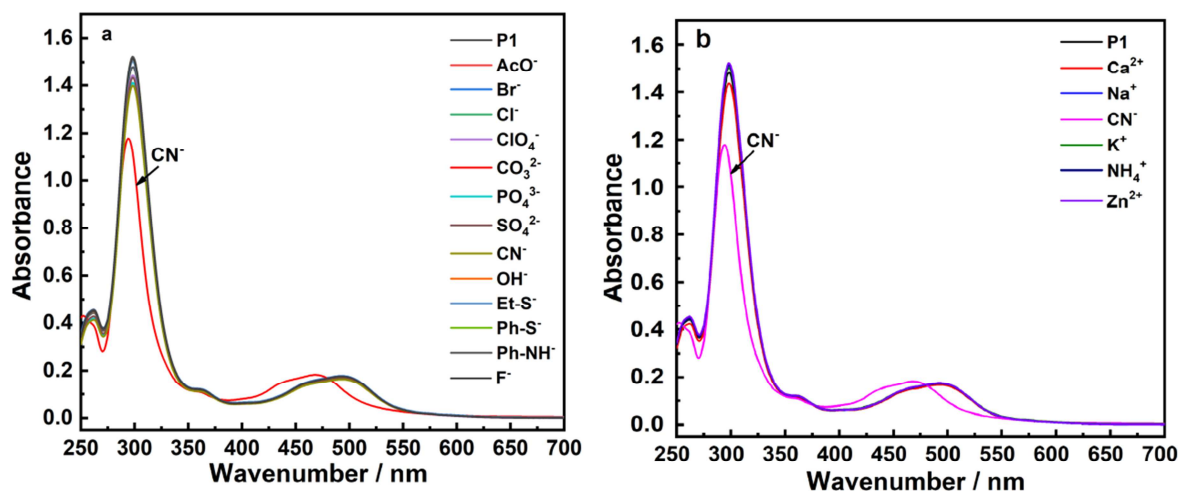


Fig. 3. UV-vis spectra of **P1** (20 μM) in the presence of 3.0 equiv. of various ions: (a) AcO^- , Br^- , Cl^- , ClO_4^- , CN^- , CO_3^{2-} , PO_4^{3-} , SO_4^{2-} , OH^- , Et-S^- , Ph-S^- , Ph-NH_2 , F^- ; (b) Ca^{2+} , Na^+ , CN^- , K^+ , NH_4^+ , Zn^{2+}) in CH_3CN .

Fluorescence spectroscopic analysis of P1. **P1** phosphorescence emission spectrum show a red-shifted, weak band at 700 nm compared with the phosphorescence spectrum of $[\text{Ru}(\text{bpy-CHO})_3](\text{PF}_6)_2$ ($\lambda_{\text{max}} = 612$ nm) [56]. This is due to the strong electron-absorbing effect of $-\text{CHO}$ in **P1**. The titration of **P1** ($\lambda_{\text{ex}} = 460$ nm) shows the gradual disappearance of the PL band at 700 nm with increasing amounts of CN^- ion and the appearance of the new band at 618 nm. This phenomenon occurs because the addition of CN^- reduces the strong electron absorption of the aldehyde groups, thereby enhancing the phosphorescence and causing blue shift ($\Delta\lambda = 100$ nm) (Fig. 4a). The phosphorescence emission intensity of the **P1** + CN^- adduct at 618 nm is plotted against the mole fraction of CN^- at a constant total concentration (20 μM). The maximum emission intensity was reached when the mole fraction of CN^- was 0.74. These results clearly indicate a 1:3 binding stoichiometry of **P1** with CN^- (Fig. 4b).

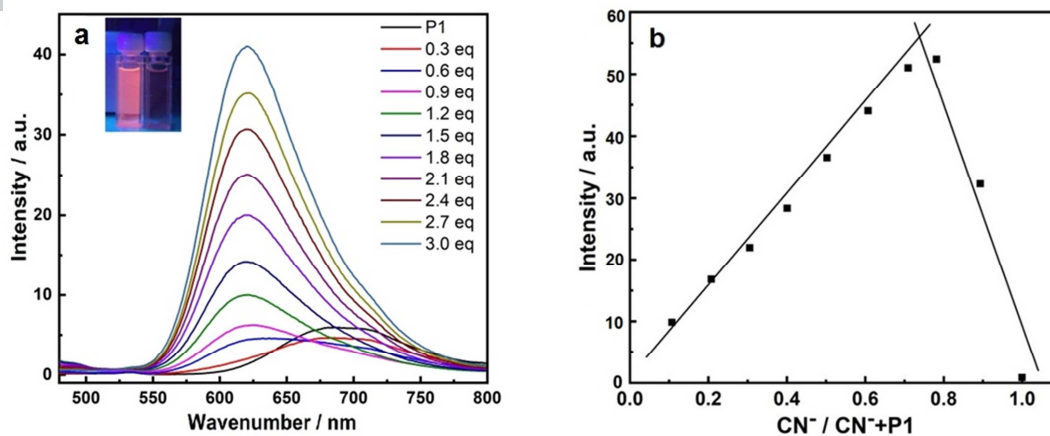


Fig. 4. (a) **P1** solution is added to the equivalent of CN^- (0.3 eq / time) phosphorescence titration (illustration left: **P1**, right: **P1** + 3CN^-). (b) Job's plots of **P1** + CN^- adduct complexes. The phosphorescence emission intensity is plotted against mole fraction of CN^- , at a constant total concentration of $20.0 \mu\text{M}$ in CH_3CN .

Reaction time of the ruthenium probe. Encouraged by the good detection of ruthenium complex with CN^- , we turned our attention on the effect of reaction time. The results were optimized shown in Fig.5. It was obvious that the PL intensity increased gradually upon addition of CN^- from 20 s and reached a maximum at about 120 s, which indicated the probe could rapidly respond to CN^- .

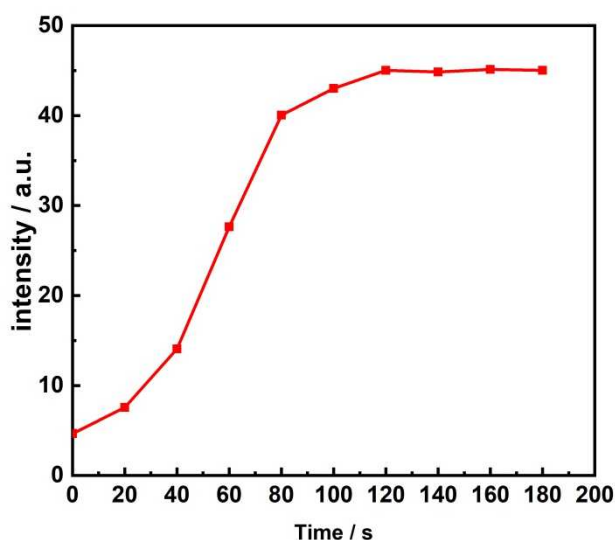


Fig. 5. Reaction time course of PL intensity of probe ($20 \mu\text{M}$) after adding 3.0 equiv. CN^- in CH_3CN at 298K ($\lambda_{\text{ex}} = 618 \text{ nm}$).

Selectivity of the probe for CN^- detection. Most of the ions used in literature for comparison are only anions, therefore, it is necessary to add cations to the contrast ions because there are not only anions in the domestic water. To evaluate the specificity of sensor towards CN^- , various ions were examined in parallel under the same conditions. No remarkable PL intensity enhancement was observed upon addition of other potentially competing anions (3.0 equiv.) to a 20 μM solution of **P1** in the absence of cyanide (Fig. 6). Reversely, adding 3.0 equivalent CN^- into **P1** in the presence of excessive anions evoke phosphorescence intensity enhancement. It is noteworthy to mention that anions such as ClO_4^- and F^- that are well-known to compete in the detection of CN^- are found to not interfere in the developed chemosensor system (Fig. 7). **P1** has much higher selectivity for CN^- than the other ions examined here. This unique property enabled CN^- to be detected directly by the naked eye over other species. Therefore, **P1** may be considered as a highly selective probe for CN^- .

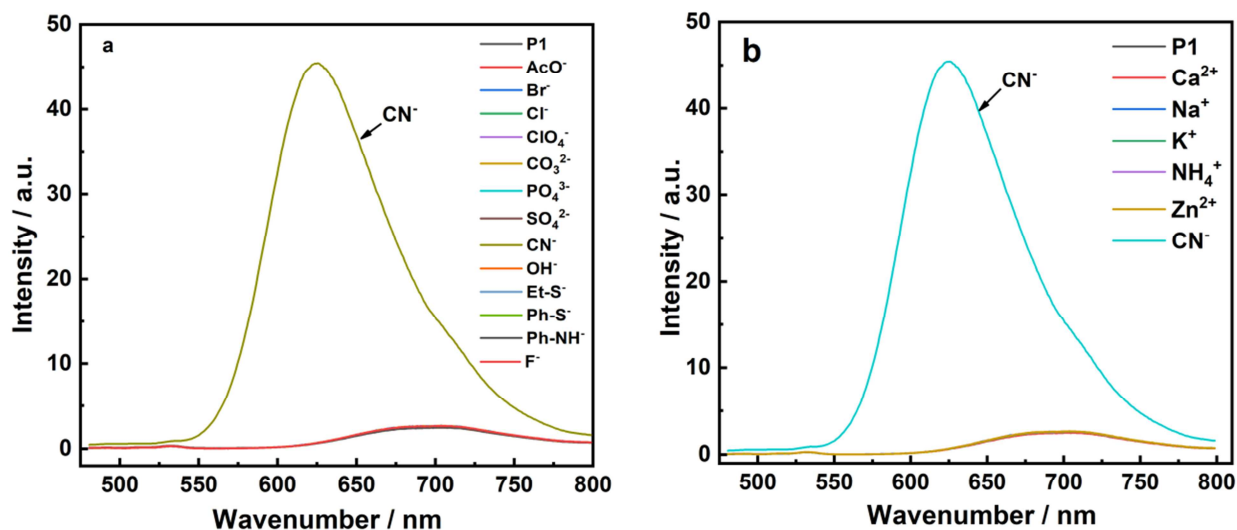


Fig. 6. PL spectra of **P1** solution with different ions ($\lambda = 460 \text{ nm}$). (a) AcO^- , Br^- , Cl^- , ClO_4^- , CN^- , CO_3^{2-} , PO_4^{3-} , SO_4^{2-} , OH^- , Et-S^- , Ph-S^- , Ph-NH_2 , F^- ; (b) Ca^{2+} , Na^+ , CN^- , K^+ , NH_4^+ , Zn^{2+} .

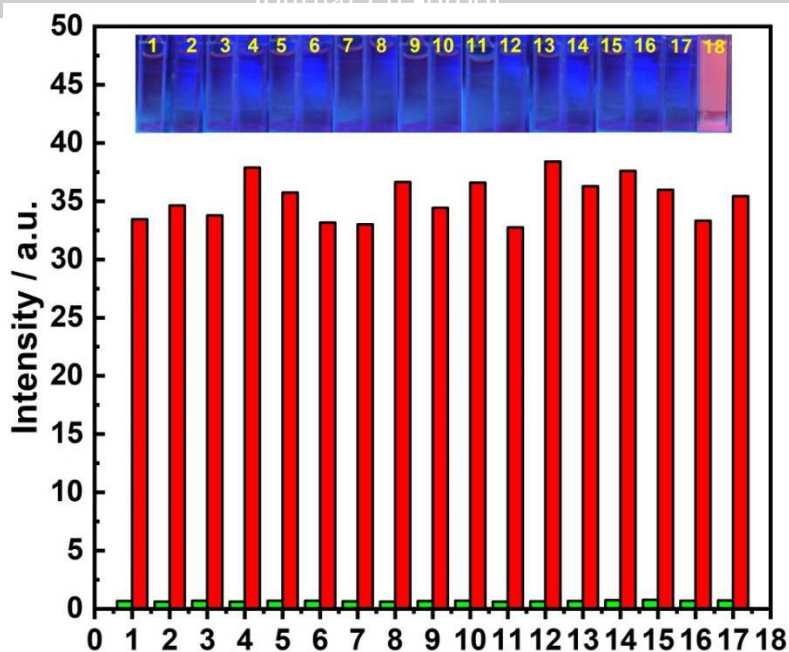


Fig. 7. Behavior of **P1** toward CN⁻ and other anions as measured by PL in acetonitrile solution (1: Ca²⁺, 2: Na⁺, 3: K⁺, 4: NH₄⁺, 5: Zn²⁺, 6: AcO⁻, 7: Br⁻, 8: Cl⁻, 9: ClO₄⁻, 10: CO₃²⁻, 11: PO₄³⁻, 12: SO₄²⁻, 13: OH⁻, 14: Et-S⁻, 15: Ph-S⁻, 16: Ph-NH₂, 17: F⁻, 18: CN⁻).

Effect of the water content. For practical use of the **P1**, PL titrations were carried out in CH₃CN / H₂O solution (60 / 40, 30 / 70 and 20 / 80 v/v) and compared with the emission properties in pure acetonitrile solution (Fig. 8). However, a maximum of ~ 7.5 equiv. CN⁻ is required to complete the reaction in 80% aqueous solution (CH₃CN / H₂O 20 / 80) that unlike the pure acetonitrile solution titration process. On the other hand, in 70% aqueous acetonitrile (CH₃CN / H₂O 30 / 70), the reaction requires a minimum of 4.5 equiv. of CN⁻. In the case of 60% aqueous acetonitrile (CH₃CN / H₂O 40 / 60) a minimum of 3.0 equiv. of CN⁻ is required for completing the reaction, which is similar to that of pure CH₃CN. This study demonstrates that the presence of water in the solution has a large effect on the reactivity of cyanide with **P1** in aqueous solution. This result is also consistent with the conclusions of the previously reported cyanide probes that the strong hydration of CN⁻ in aqueous solution reduces its nucleophilicity. Further, the phosphorescence titration data of different water contents were plotted, and it was found that pure acetonitrile and 60% aqueous

acetonitrile solution were basically the same in the growth trend under the same conditions. The phosphorescence growth trend of other water contents is slower than that of pure acetonitrile especially 80% water acetonitrile solution ($\text{CH}_3\text{CN} / \text{H}_2\text{O} 20 / 80$), which requires not only up to 7.5 equiv. of CN^- to achieve the phosphorescence intensity of pure acetonitrile solution but also a much lower growth trend. Therefore, it can be concluded from these studies that **P1** is selective and sensitive to CN^- in aqueous solution (60% water), which makes **P1** possible as a probe for detecting CN^- in practical applications.

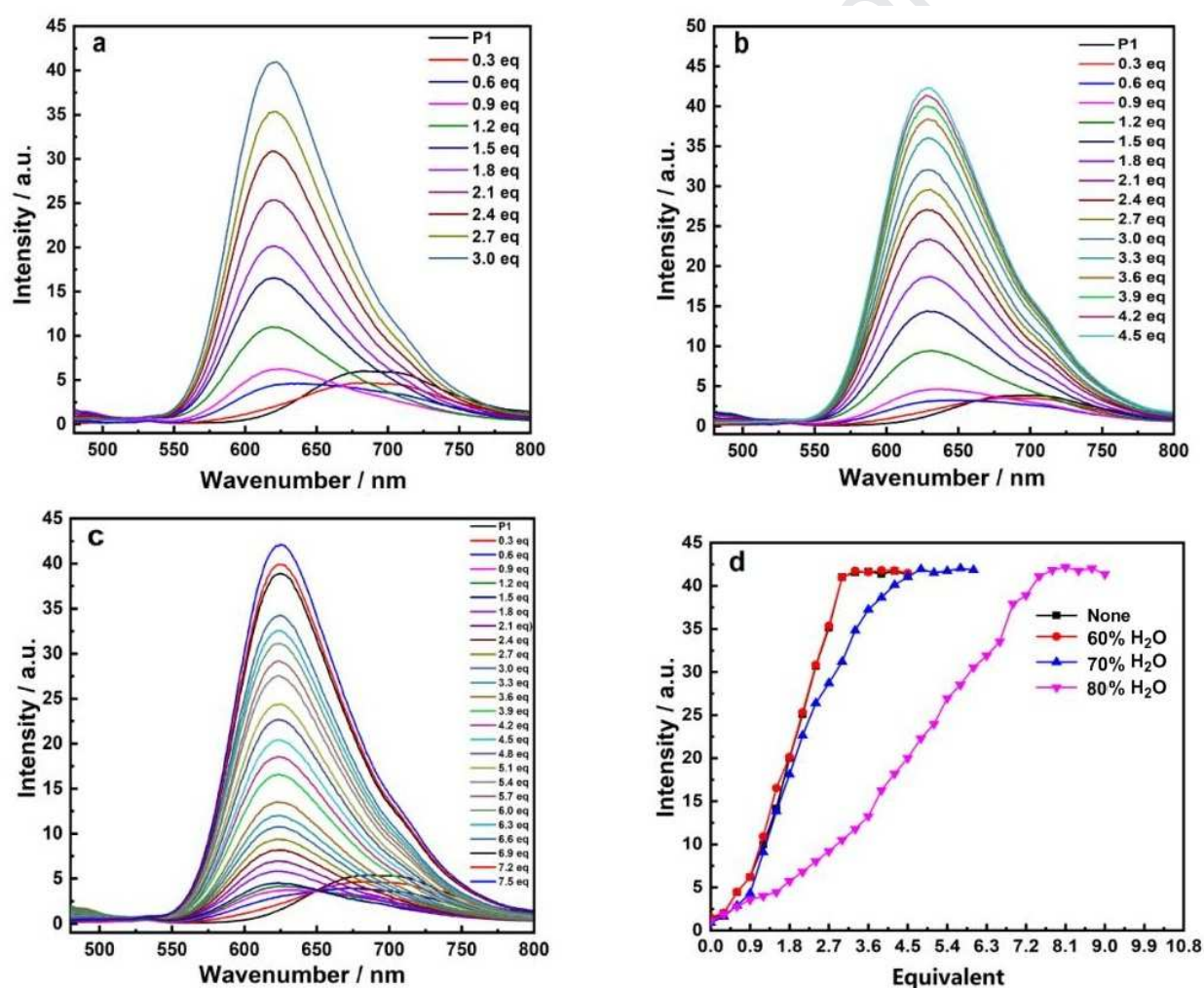


Fig. 8. Titration image of **P1** in different aqueous solutions. (a) $\text{CH}_3\text{CN} / \text{H}_2\text{O} (50 / 50)$; (b) $\text{CH}_3\text{CN} / \text{H}_2\text{O} (40 / 60)$; (c) $\text{CH}_3\text{CN} / \text{H}_2\text{O} (30 / 70)$; (d) **P1** titrated in different water content solutions phosphorescence growth trend.

The determination limit was detected CN⁻ in the Solution State. The detection limit is one of the important criteria to judge the performance of the probe. Recently, the detection limit of both pure organic fluorescent probes and organic metal fluorescent probes in the detection of related ions is getting lower and lower. In table 1, the detection limits of pure organic phosphorescence and organometallic fluorescent probes with certain representativeness in detecting CN⁻ in recent years are listed. The detection limits in the table are large and small but the overall trend shows a decrease. The detection limit of **P1** for CN⁻ was calculated based on the phosphorescence titration data according to a reported method [57]. Under optimal conditions, calibration graphs for the determination of CN⁻ were constructed. The decreased phosphorescence intensity of the system showed a good linear relationship ($r = 0.991$), as shown in Fig. 9. The limit of detection (LOD) was calculated to be 0.75 μM on the basis of $S / N = 3$, which is far lower than the permissible limit (1.9 mM) set by the WHO

Table 1. Detection limit of cyanide for different types of probes

Compound	Solvent	LOD / μM
RuL1-CuL2 [58]	DMF / H ₂ O (5 / 5)	1.20
L [59]	CH ₃ CN / H ₂ O (6 / 4)	0.50
3 [60]	H ₂ O	0.28
Probe 1 [61]	THF	0.67
GSB [62]	DMSO / H ₂ O (9 / 1)	0.88
3TBN [63]	DMSO / H ₂ O (9 / 1)	0.46
S1 [64]	MeOH / H ₂ O (5 / 5)	3.60
P1	CH ₃ CN / H ₂ O (6 / 4)	0.75

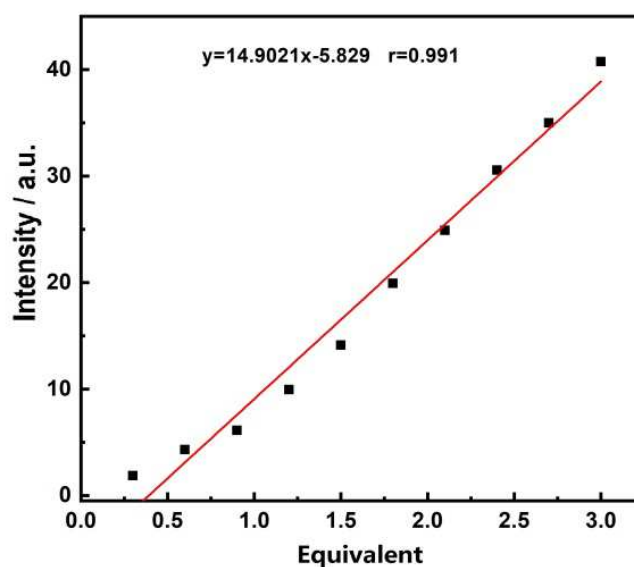


Fig. 9. P1 (20 μM) as a probe for calibration of CN^- luminescence detection

Preparation of Filter Paper Test Strips. Motivated by the favorable features of **P1** as a potential probe for CN^- in solution, we have prepared luminescent test strips using **P1** for the detection of CN^- anions by contact mode. The ordinary filter paper (1.8cm \times 2.0 cm) was immersed in **P1** solution (20 μM) for 5 minutes and then removed to dry naturally. A series of CN^- solution of different concentrations (5000–0.5 μM) was configured and 2 μL was dropped on the filter paper and data were collected, all of which was shown in Fig. 10. Small spots of CN^- solution of different concentrations were generated on the test strip impregnated with **P1**. The color of the test strip with concentration of a drop of 50 μM could still be clearly observed to change from orange to pale yellow by naked eyes. When excited with 365nm, the test strip with the drop of CN^- solution showed red fluorescent spots, even though the concentration was 5 μM . The test results demonstrate the practical utility of the **P1** impregnated test strips for the instant on-site visualization of trace amounts of cyanide ions present in solution by the naked eye and the 365 nm [65].

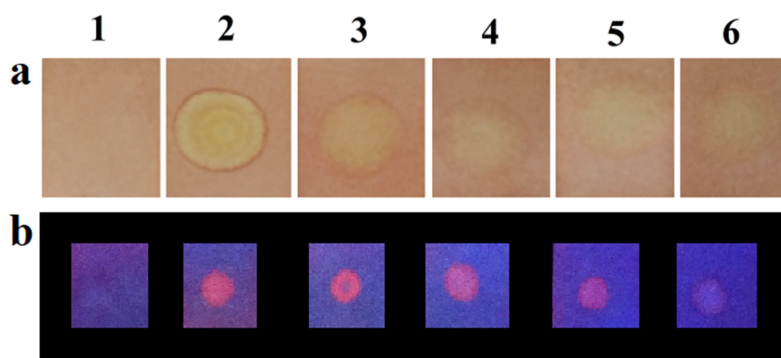
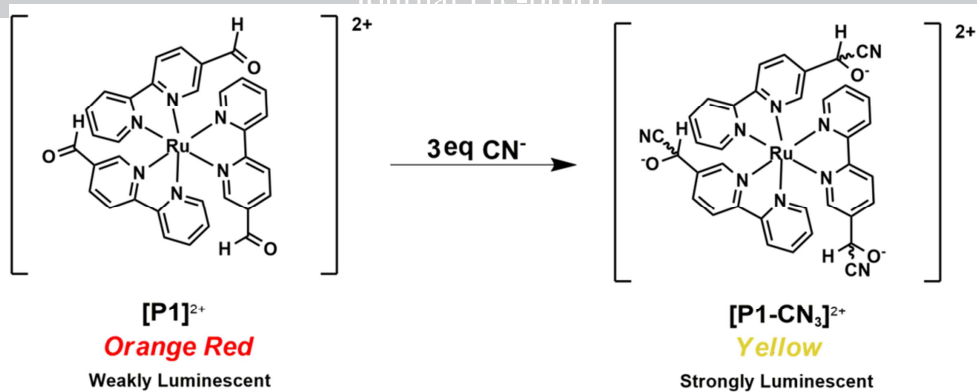


Fig. 10. Plot of the emission intensity at (a) visible light and (b) 365 nm of the test strips against concentration of added CN^- in acetonitrile (1: blank, 2: 5000 μM , 3: 500 μM , 4: 50 μM , 5: 5 μM , 6: 0.5 μM , The same below).

Confirmation of the generation of cyanohydrins. The formation of cyanohydrin was further confirmed by ^1H NMR and FT-IR spectroscopy. Nuclear magnetic profiling of the reaction of aldehyde groups with cyanide ions is well described in many articles. Khatua [55] studied the change of aldehyde group and CN^- binding by nuclear magnetic titration. It narrated the change of proton peak in the reaction between aldehyde group and CN^- and proposed that the early disappearance of aldehyde matrix hydrogen is due to the possibility of hydration. Fig. 11 shows during the addition of **P1** with 3.0 equiv of CN^- the intensity of the sharp singlet at δ 9.96 ppm corresponding to the aldehyde protons immediate disappearance and upfield shifts are noted for the formylated pyridyl ring protons of the ligand. All of the ligand proton hydrogen signals besides the cyanohydrin protons move toward the upfield [66]. In addition, results obtained from ESI-HRMS spectra were consistent with that of ^1H NMR spectra. The corresponding characteristic peaks of cyanohydrins were found in the mass spectra of **P1** with CN^- in different molar ratios (**P1** : CN^- = 1:1; 1:2; 1:3; respectively) (Fig.S9–S11 in ESI).



Scheme 2. Cyanide detection by **P1** based on cyanohydrins formation.

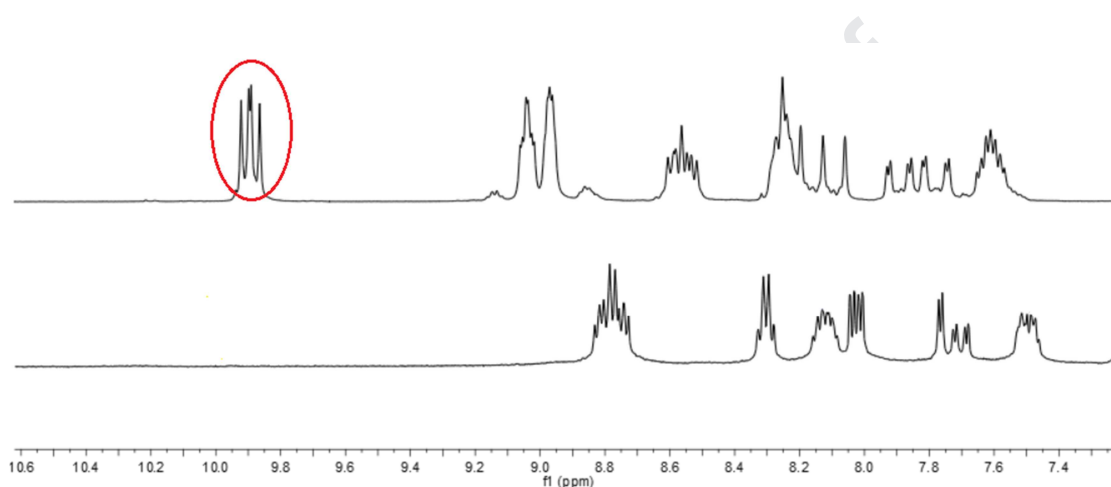


Fig. 11. Partial ^1H NMR spectra show the changes of **P1** and **P1** + 3.0 eq. CN^- in d_6 -DMSO at room temperature.

The FT-IR spectrum clearly indicates the appearance of the cyanogen group stretching frequency ($\sim 2170 \text{ cm}^{-1}$) and disappearance of the carbonyl frequency of stretching ($\sim 1700 \text{ cm}^{-1}$) of the aldehyde group in **P1**. On the basis of the results from ^1H NMR chemical shifts, mass spectra and FT-IR spectroscopy, the most plausible mechanism for the formation of the cyanide adducts (cyanohydrin) was proposed. The strong electron-deficient properties of the $-\text{CHO}$ group in **P1** make it susceptible to nucleophilic attack by CN^- , while the carbonyl group is attacked by the formation of cyanohydrin, a very stable adduct that makes the reaction completely irreversible [67, 68].

Conclusions

In summary, a new ruthenium complex (**P1**) has been prepared to detect cyanide based on a cyanohydrin chemodosimeter reaction. The immediate color change from orange-red to yellow and orange luminescence can be observed by the naked eye after CN^- addition. The probe upon interaction with different cation and anion showed high selectivity and sensitivity for CN^- through phosphorescence “turn-on” response in aqueous solution (60 % water) with a detection limit of 0.75 μM . Phosphorescent test strips have been fabricated and utilized for the detection of micromole levels of cyanide in mixed aqueous solution. Finally, the formation of cyanohydrin has been further corroborated by ^1H NMR, FT-IR and mass spectral studies.

Experimental Section

All manipulations were performed under an atmosphere of nitrogen using standard Schlenk techniques. Chemicals were used as commercial products without further purification. ^1H NMR (500 MHz) spectra were recorded with a Bruker DMX-500 spectrometer. Elemental analysis was performed on an Elementar vario EL III analyzer. IR (KBr) spectra were recorded with the Nicolet FT-IR spectrophotometer.

The **P1** solution used in phosphorescence titration and UV-vis titration is composed of specpure acetonitrile as the solvent, and the anion and cation solutions are used as the solvent of acetonitrile : water (60 / 40), the corresponding salts are used as the solute. To reduce the interference of the anion and cation solvents, the concentration of all anions and cations is 100 μM , and The concentration of the transparent solution of **P1** is 20 μM . Waiting for 3 minutes after each equal amount of ion solution is added to make the data accurate and the excitation wavelength is $\lambda = 460$ nm.

Synthesis of 5-aldehyde-2, 2'-bipyridine(CHO-bpy) L1. Pd(PPh₃)₂Cl₂ (52.0 mg, 0.08 mmol), PPh₃ (38.5mg, 0.15 mmol), 2-(tributylstannylpyridine) (552.2 mg, 1.50 mmol), 6-bromo-3-pyridinecarbaldehyde (329.0 mg, 1.77 mmol) and toluene (20.0 mL) were added to an oven-dried Schlenk flask. The resulting mixture was stirred for 72 h under N₂ atmosphere. Then the reaction mixture was cooled to room temperature and the solvent was removed under reduced pressure. The obtained solid was dissolved in CH₂Cl₂ (25.0 mL) and washed with a saturated NH₄Cl solution (15.0 mL). The aqueous phase was extracted with CH₂Cl₂. The organic layers were combined, the solvent was removed under reduced pressure and the crude product was purified by silica gel column chromatography (EA / PE = 3 / 7) to give L1 as a white solid. Yield: 47 % (130.0 mg), mp: 223 °C (76 mmHg), IR (KBr): 1699, 1584, 1553, 1445, 1250, 1034, 846 cm⁻¹. ¹H NMR (500 MHz, CDCl₃): δ 10.17 (1H, s), 9.13 (1H, s), 8.73 (1H, d, *J* = 3.9 Hz), 8.61 (1H, d, *J* = 8.2 Hz), 8.51 (1H, d, *J* = 7.9 Hz), 8.29 (1H, dd, *J* = 8.2, 3.5 Hz), 7.87 (1H, t, *J* = 7.0 Hz), 7.42–7.36 (1H, m), ¹³C NMR (125 MHz, CDCl₃): δ 190.9, 160.8, 154.7, 151.8, 149.5, 137.5, 137.2, 131.2, 125.0, 122.4, 121.5 ppm, HRMS calcd [M+H]⁺: *m/z* 185.0715; found: 185.0712, Elemental analysis calcd (%) for C₁₁H₈N₂O: C 71.73, H 4.38, N 15.21; found: C 71.65, H 4.40, N 15.30. ¹H and ¹³C NMR data are in agreement with those published [69].

Synthesis of [Ru(CHO-bpy)₃](PF₆)₂ P1. 64.4 mg of L1 (0.35 mmol) in 15 mL of EtOH was added to a solution of RuCl₃ (20.7 mg, 0.10 mmol) in 20 mL of EtOH / H₂O (3 / 1). The reaction mixture was refluxed for 24 h, and then cooled to room temperature. After the solvent was evaporated, the residue was dissolved in a small amount of water, and then the aqueous solution was washed with CH₂Cl₂. A saturated solution of NH₄PF₆ was added to yield red precipitate of the product, which was further purified by neutral aluminum oxide column chromatography with CH₂Cl₂ / MeOH (10 / 1) as eluent. The target Ru(II) complex P1 was isolated as a red solid. Yield: 54 % (53.0 mg), mp:

469 °C (76 mmHg), IR (KBr): 1761, 1623, 1583, 1423, 1295, 810 cm^{-1} , ^1H NMR (500 MHz, d_6 -DMSO) δ 9.89 (3H, dd, $J = 5.0, 2.5$ Hz), 9.03 (3H, s), 8.97 (3H, s), 8.56 (3H, t, $J = 5.0$ Hz), 8.16 (6H, dd, $J = 5.0, 2.5$ Hz), 7.83 (3H, dd, $J = 5.0, 2.5$ Hz), 7.61 (3H, s), ^{13}C NMR (125 MHz, d_6 -DMSO): δ 190.9, 160.9, 156.2, 151.5, 149.3, 138.8, 133.6, 129.3, 126.4, 126.2, 125.1 ppm, HRMS calcd $[\text{M-PF}_6]^+$: m/z 799.0595; found: 799.0587, Elemental analysis calcd (%) for $\text{C}_{33}\text{H}_{24}\text{F}_{12}\text{N}_6\text{O}_3\text{P}_2\text{Ru}$: C 42.01, H 2.56, N 8.91; Found: C 42.15, H 2.47, N 8.78.

X-ray Crystallography. Diffraction data of **P1** were collected on a Bruker Smart APEX CCD diffractometer with graphite-monochromated MoK α radiation ($\lambda = 0.71073$ Å). All the data were collected at room temperature, and the structures were solved by direct methods and subsequently refined on F^2 by using full-matrix least-squares techniques (SHELXL). SADABS absorption corrections were applied to the data, all non-hydrogen atoms were refined anisotropically, and hydrogen atoms were located at calculated positions. All calculations were performed using the Bruker program Smart.

Supporting Information

Electronic supplementary information (ESI) available: ^1H NMR spectra of ligand and ruthenium complex; FT-IR spectra of complex. CCDC 1956947 contains the supplementary crystallographic data for this paper. These data can be obtained free of charge via www.ccdc.cam.ac.uk/data_request/cif.

Conflicts of Interest

The authors declare no competing financial interests.

Acknowledgements

This work was supported by the National Natural Science Foundation of China (No. 21601125), the Chenguang Scholar of Shanghai Municipal Education Commission (No. 16CG64), the Shanghai Gaofeng & Gaoyuan Project for University Academic Program Development, and the Industry Catalysis Funding of Shanghai Institute of Technology (CHJJ-2).

References

- [1] Beer PD, Gale PA. Anion Recognition and Sensing: The State of the Art and Future Perspectives. *Angew Chem Int Ed* 2001; 40: 486–516.
- [2] Yoon J, Kim SK, Singh NJ, Kim KS. Imidazolium receptors for the recognition of anions. *Chem Soc Rev* 2006; 35: 355–360.
- [3] Gunnlaugsson T, Glynn M. Anion recognition and sensing in organic and aqueous media using luminescent and colorimetric sensors. *Chem Rev* 2006; 250: 3094–3117.
- [4] Xu Z, Chen X, Kim HN. ChemInform Abstract: Sensors for the Optical Detection of Cyanide Ion. *Chem Soc Rev* 2010; 39: 127–137.
- [5] Jun ME, Roy B, Ahn KH. “Turn-on” fluorescent sensing with “reactive” probes. *Chem Commun* 2011; 47: 7583–7601.
- [6] Xu Z, Pan J, Spring DR. Cui J, Yoon J. Ratiometric fluorescent and colorimetric sensors for Cu^{2+} based on 4,5-disubstituted-1,8-naphthalimide and sensing cyanide via Cu^{2+} displacement approach. *Tetrahedron* 2010; 66: 1678–1683.
- [7] Cui JX, Chen X, Guan LP, Tang XL, Wang CM, Meng Y, et al. Ratiometric Iridium(III) Complex-Based Phosphorescent Chemodosimeter for Hg^{2+} Applicable in Time-Resolved Luminescence Assay and Live Cell Imaging. *Anal Chem* 2015; 87: 3255-3262.
- [8] Ru JX, Tang XL, Ju ZH, Zhang GL, Dou W, Mi XQ, Wang CM, Liu WS. Exploitation and Application of a Highly Sensitive Ru(II) Complex-Based Phosphorescent Chemodosimeter for Hg^{2+}

in Aqueous Solutions and Living Cells. *ACS Appl Mater Interfaces* 2015; 7: 4247–4256.

[9] Zhang YY, Zhou QX, Tian N, Li C, Wang XS. Ru(II)-Complex-Based DNA Photocleaver Having Intense Absorption in the Phototherapeutic Window. *Inorg Chem* 2017; 56: 1865–1873.

[10] Yamamoto Y, Tamaki Y, Yui T, Koike K, Ishitani O. New Light-Harvesting Molecular Systems Constructed with a Ru(II) Complex and a Linear-Shaped Re(I) Oligomer. *J Am Chem Soc* 2010;132: 11743–11752.

[11] Yamazaki Y, Ohkubo K, Saito D, Yastu T, Tamaki Y, Tanaka S, et al. Kinetics and Mechanism of Intramolecular Electron Transfer in Ru(II)–Re(I) Supramolecular CO₂-Reduction Photocatalysts: Effects of Bridging Ligands *Inorg Chem* 2019; 58: 11480–11492.

[12] Lameijer LN, Griend CVD, Hopkins SL, Volbeda AG, Askes SHC, Siegler MA, Bonnet S. Photochemical Resolution of a Thermally Inert Cyclometalated Ru(phbpy)(N-N)(Sulfoxide)⁺ Complex. *J Am Chem Soc* 2019; 141: 352–362.

[13] Sun W, Zeng XL, Wu S. Cucurbit[6]uril-based multifunctional supramolecular assemblies: Synthesis removal of Ba(II) and fluorescence sensing of Fe(III). *Dalton Trans* 2018; 47: 3958–3964.

[14] Fabbrizzi L, Licchelli M, Rabaioli G, Taglietti A. The Design of Luminescent Sensors for Anions and Ionisable Analytes. *Chem Rev* 2000; 205: 85–108.

[15] Steed JW. Coordination and organometallic compounds as anion receptors and sensors. *Chem Soc Rev* 2009; 38: 506–519.

[16] Bomben PG, Robson KCDP. On the Viability of Cyclometalated Ru(II) Complexes for Light-Harvesting Applications. *Inorg Chem* 2009; 48: 9631–9643. (b) Hagfeldt A, Boschloo G. Dye-Sensitized Solar Cells, *Chem Rev* 2010; 110: 6595–6663.

[17] Robson KCD, Koivisto BD. Design and Development of Functionalized Cyclometalated Ruthenium Chromophores for Light-Harvesting Applications. *Inorg Chem* 2011; 50: 5494–5508.

- [18] Khatua S, Sheet SK, Sen B. Cationic Organoiridium(III) Complex Based AIEgen for Selective Light up Detection of rRNA and Nucleolar Staining. *Dalton Trans* 2018; 10: 1039.
- [19] Badjic JD, Ronconi CM. Operating Molecular Elevators Operating Molecular Elevators. *J Am Chem Soc* 2006; 128: 1489–1499.
- [20] Petitjean A, Puntoriero F. Synthesis Optical and Electronic Properties of Bridged Bis \square dirhodium and \square diruthenium Complexes. *Eur J Inorg Chem* 2010; 2006: 3878–3892.
- [21] Balzani V, Bergamini G, Marchioni F. Ru(II)-bipyridine complexes in supramolecular systems devices and machines. *Chem Rev* 2006; 250: 1254-1266.
- [22] Zhu LB, Yang QB. Reaction-based fluorescent probe for differential detection of cyanide and bisulfite in the aqueous media. *J Lumin* 2019; 215: 116620.
- [23] Liu F, Concepcion JJ, Jurss JW, Cardolaccia T, Templeton JL, Meyer JL. Mechanisms of Water Oxidation from the Blue Dimer to Photosystem II. *Inorg Chem* 2008; 47: 1727–1752.
- [24] Fan Y, Zhang LY, Dai FR, Shi LX, Chen ZN. Preparation Characterization and Photophysical Properties of Pt-M (M = Ru Re) Heteronuclear Complexes with 1,1'-Phenanthrolineethynyl Ligands. *Inorg Chem* 2008; 47: 2811–2819.
- [25] Zhao S, Arachchige SM, Slebodnick C, Brewer KJ. Synthesis and Study of the Spectroscopic and Redox Properties of Ru(II) Pt(II) Mixed-Metal Complexes Bridged by 2,3,5,6-Tetrakis(2-pyridyl)pyrazine. *Inorg Chem* 2008; 47: 6144–6152.
- [26] Shiotsuka M, Nishiko N, Keyak K, Nozaki K. Construction of a photoactive supramolecular system based on a platinum(II) bis-acetylide building block incorporated into a ruthenium(II) polypyridyl complex. *Dalton Trans* 2010; 39: 1831–1835.
- [27] Wong KMC, Yam VWW. Luminescence platinum(II) terpyridyl complexes—From fundamental studies to sensory functions. *Chem Rev* 2007; 251: 2477–2488.

- [28] Zhao Q, Li F. Phosphorescent chemosensors based on heavy-metal complexes. *Chem Soc Rev* 2010; 39: 3007–3030.
- [29] Wanatabe S, Ikishima SA. Luminescent Metalloreceptor Exhibiting Remarkably High Selectivity for Mg^{2+} over Ca^{2+} . *J Am Chem Soc* 2001; 123: 8402–8403.
- [30] McFarland SA, Finney NS. Modulating the efficiency of Ru(II) luminescence via ion binding-induced conformational restriction of bipyridyl ligands. *Chem Commun* 2003; 388–389.
- [31] Ghosh A, Ganguly B, Das A. Urea-Based Ruthenium(II)-Polypyridyl Complex as an Optical Sensor for Anions: Synthesis Characterization and Binding Studies. *Inorg Chem* 2007; 46: 9912–9918.
- [32] Cui Y, Mo HJ, Chen JC, Niu YL, Zhong YR, Zheng KC, Ye BH. Anion-Selective Interaction and Colorimeter by an Optical Metalloreceptor Based on Ruthenium(II) 2,2'-Biimidazole: Hydrogen Bonding and Proton Transfer. *Inorg Chem* 2007; 46: 6427–6436.
- [33] Cui Y, Niu YL, Cao ML, Wang K, Mo HJ, Zhong YR, Ye BH. Ruthenium(II) 2,2'-Bibenzimidazole Complex as a Second-Sphere Receptor for Anions Interaction and Colorimeter. *Inorg Chem* 2008; 47: 5616–5624.
- [34] McGee KA, Mann KR. Inefficient Crystal Packing in Chiral $[Ru(phen)_3](PF_6)_2$ Enables Oxygen Molecule Quenching of the Solid-State MLCT Emission. *J Am Chem Soc* 2009; 131: 1896–1902.
- [35] Payne SJ, Fiore GL, Fraser CL, Demas JN. Luminescence Oxygen Sensor Based on a Ruthenium(II) Star Polymer Complex *Anal Chem* 2010 82 917–921
- [36] Ji S Wu W Wang Z Liu S Guo H Zhao J Tuning the luminescence lifetimes of ruthenium(II) polypyridine complexes and its application in luminescent oxygen sensing. *J Mater Chem* 2010; 20: 1953–1963.

- [37] Zhang J, Qi H, Li Y, Yang J, Gao Q, Zhang C. Electrogenated Chemiluminescence DNA Biosensor Based on Hairpin DNA Probe Labeled with Ruthenium Complex. *Anal Chem* 2008; 80: 2888–2894.
- [38] Aoki S, Zulkefeli M, Shiro M, Kohsako M, Takeda K, Kimura E. A Luminescence Sensor of Inositol 1,4,5-Triphosphate and Its Model Compound by Ruthenium-Templated Assembly of a Bis(Zn^{2+} -Cyclen) Complex Having a 2,2'-Bipyridyl Linker (Cyclen = 1,4,7,1'-Tetraazacyclododecane). *J Am Chem Soc* 2005; 127: 9129–9139.
- [39] Zhang R, Yu X, Ye Z, Wang G. Turn-on Luminescent Probe for Cysteine / Homocysteine Based on a Ruthenium(II) Complex. *Inorg Chem* 2010; 49: 7898–7903.
- [40] Kim YK, Lee YH, Lee HY, Kim MK, Cha GS, Ahn KH. Molecular Recognition of Anions through Hydrogen Bonding Stabilization of Anion-Ionophore Adducts: A Novel Trifluoroacetophenone-Based Binding Motif. *Org Lett* 2003; 5: 4003–4006.
- [41] Lee KS, Kim HJ, Kim GH, Shin I, Hong JI. Fluorescent Chemodosimeter for Selective Detection of Cyanide in Water. *Org Lett* 2008 10 49–51
- [42] Cho D G Kim J H Sessler J L The Benzil–Cyanide Reaction and Its Application to the Development of a Selective Cyanide Anion Indicator. *J Am Chem Soc* 2008; 130: 12163–12167.
- [43] Sessler JL, Cho DG. The Benzil Rearrangement Reaction: Trapping of a Hitherto Minor Product and Its Application to the Development of a Selective Cyanide Anion Indicator. *Org Lett* 2008; 10: 73–75.
- [44] Hong SJ, Yoo J, Kim SH, Kim JS, Yoon J, Lee CH. Pyrophosphate selective fluorescent chemosensors based on coumarin–DPA–Cu(II) complexes. *Chem Commun* 2009; 189–191.
- [45] Kim DS, Chung YM, Jun M, Ahn KH. Selective Colorimetric Sensing of Anions in Aqueous Media through Reversible Covalent Bonding. *J Org Chem* 2009; 74: 4849–4854.

- [46] Otte M, Kuijpers PF, Troeppner OJ. Back Cover: Encapsulation of Metalloporphyrins in a Self-Assembled Cubic M_8L_6 Cage: A New Molecular Flask for Cobalt-Porphyrin-Catalysed Radical-Type Reactions. *Chem Eur J* 2013; 19: 10420–10420.
- [47] Poeller S, Schuhmann W. Visualization of electrocatalytic activity of microstructured metal hexacyanoferrates by means of redox competition mode of scanning electrochemical microscopy. *Electrochim Acta* 2014; 140: 101–107.
- [48] Zoppellaro G, Ivanova A, Enkelmann V. Synthesis magnetic properties and theoretical calculations of novel nitronyl nitroxide and imino nitroxide diradicals grafted on terpyridine moiety. *Polyhedron* 2003; 22: 2099–2110.
- [49] Zhang R, Yu X, Ye Z. Turn-on Luminescent Probe for Cysteine / Homocysteine Based on a Ruthenium(II) Complex. *Inorg Chem* 2010; 49: 7898–7903.
- [50] Yao ZJ, Zhu JW, Lin N, Qiao XC, Deng W. Catalytic Hydrogenation of Carbonyl and Nitro Compounds Using [NO]-chelate Half-Sandwich Ruthenium Catalyst. *Dalton Trans* 2018; 10: 1039.
- [51] Ito A, Kobayashi N, Teki Y. Low-Energy and Long-Lived Emission from Polypyridyl Ruthenium(II) Complexes Having A Stable-Radical Substituent. *Inorg. Chem.* 2017; 56: 3794–3808.
- [52] Barnsley EJ, Findlay AJ, Shillito EG, Pelet S W, Scottwell ØS, et al. Long-lived MLCT states for Ru(II) complexes of ferrocene-appended 2,2'-bipyridines. *Dalton Trans.* 2019; 48: 15713–15722
- [53] Silverstein WD, Milojevich BC, Camden PJ, Jensen L. Investigation of Linear and Nonlinear Raman Scattering for Isotopologues of $Ru(bpy)_3^{2+}$. *J Phys Chem. C.* 2013; 117: 20855–20866.
- [54] Klein S, Dougherty GW, Kassel WS, Dudley JT, Paul JJ. Structural, Electronic, and Acid / Base Properties of $[Ru(bpy)_2(bpy(OH)_2)]_2$ ($bpy = 2,2'$ -Bipyridine, $bpy(OH)_2 = 4,4'$ -Dihydroxy-

2,2'-bipyridine). *Inorg Chem.* 2011; 50: 2754–2763.

[55] Khatua S, Samanta D, Bats JW, Schmittel M. Rapid and Highly Sensitive Dual-Channel Detection of Cyanide by Bis-heteroleptic Ruthenium(II) Complexes. *Inorg Chem* 2012; 51: 7075–7086.

[56] Chen LF, Doeven EH, Wilson DJD, Kerr E, Hayne DJ, Hogan CF, et al. Co-reactant Electrogenerated Chemiluminescence of Iridium(III) Complexes Containing an Acetylacetonate Ligand. *Chem Electro Chem* 2017; 4: 1797–1808.

[57] Tong CL, Xiang GH. Sensitive determination of enoxacin by its enhancement effect on the fluorescence of terbium(III)–sodium dodecylbenzene sulfonate and its luminescence mechanism. *J Lumin* 2007;126: 575–580.

[58] Chow CF, Wong WY. A Heterobimetallic Ruthenium(II)-Copper(II) Donor-Acceptor Complex as a Chemodosimetric Ensemble for Selective Cyanide Detection. *Inorg Chem* 2004; 43: 8387.

[59] Maji S, Ghosh P. Ruthenium(II) complexes containing the pentadentate SNNNS chelating ligand 2,6-diacetylpyridine bis(4-(p-tolyl)thiosemicarbazone) Synthesis reactivity and electrochemistry. *Inorg Chim Acta* 2018; 483: 321–328.

[60] Agarwalla H, Gangopadhyay M, Sharma DK, Basu SK, Jadhav S, Chowdhury A, et al. Fluorescent probes for the detection of cyanide ions in aqueous medium: cellular uptake and assay for b-glucosidase and hydroxynitrile lyase. *J Mater Chem, B* 2015; 3: 9148.

[61] Wang LY, Zhuo SC, Cao DR. A Colorimetric and Fluorescent Probe Based on Michael Acceptor Type Diketopyrrolopyrrole for Cyanide Detection. *J Fluoresc* 2017; 27: 1587–1594.

[62] Sukato R, Wacharasindhu S, Sangpetch N, Palaga T. New Turn-On Fluorescent and Colorimetric Probe for Cyanide Detection Based on BODIPY-Salicylaldehyde and its Application in Cell Imaging. *J Hazard Mater* 2016; 314: 277–285.

- [63] Niu QF, Lan LX, Li TD, Guo ZR, Jiang T, Zhao ZY, et al. A highly selective turn-on fluorescent and naked-eye colorimetric sensor for cyanide detection in food samples and its application in imaging of living cells. *Sensor Actuat B: Chem* 2018; 276: 13–22.
- [64] Rao PG, Rao TS. Highly selective reaction based colorimetric and fluorometric chemosensors for cyanide detection via ICT off in aqueous solution. *J Photoch & Photobio A: Chem* 2019; 372: 177–185.
- [65] Bejoymohandas KS, Kumar A, Sreenadh S, Varathan E, Varughese S, Reddy MLP. A Highly Selective Chemosensor for Cyanide Derived from a Formyl-Functionalized Phosphorescent Iridium(III) Complex. *Inorg Chem* 2016; 55: 3448–3461.
- [66] Moghadam FN, Amirnasr M, Eskandari K, Meghdadi S. A new disulfide Schiff base as a versatile “OFF–ON–OFF” fluorescent–colorimetric chemosensor for sequential detection of CN^- and Fe^{3+} ions: combined experimental and theoretical studies. *New J Chem* 2019; 43: 13536.
- [67] Yadav N, Singh AK. Dicarbohydrazide based chemosensors for copper and cyanide ions via a displacement approach. *New J Chem* 2018; 42: 6023.
- [68] Kodlady SN, Narayana B, Sarojini BK, Gauthama BU. Aromatic aldehyde based chemosensors for fluoride and cyanide detection in organic and aqueous media: Ascertained by characterization spectroscopic and DFT studies. *Inorg Chim Acta* 2019; 494: 245–255.
- [69] Citta A, Scalcon V, Göbel P, Bertrand B, Wenzel M, Folda A, Rigobello MP, Meggers E, Casini A. Toward anticancer gold-based compounds targeting PARP-1: a new case study. *RSC Adv.* 2016; 6: 79147–79152.

**Ruthenium-based phosphorescent probe for selective and naked-eye
detection of cyanide in aqueous media**

Jing-Wei Zhu,^a Hui-Dan Ou,^a Niwei Xu,^c Wei Deng,^{*a} Zi-Jian Yao^{*a, b}

^a School of Chemical and Environmental Engineering, Shanghai Institute of Technology, Shanghai, 201418, China.

^b State Key Laboratory of Chemo/Biosensing and Chemometrics, Hunan University, Changsha 410082, China

^c Hunan Traditional Chinese Medical College, Zhuzhou, 412012, China

Corresponding author: Email: zjyao@sit.edu.cn; Tel: +86-21-60877231, Fax: +86-21-60873335.

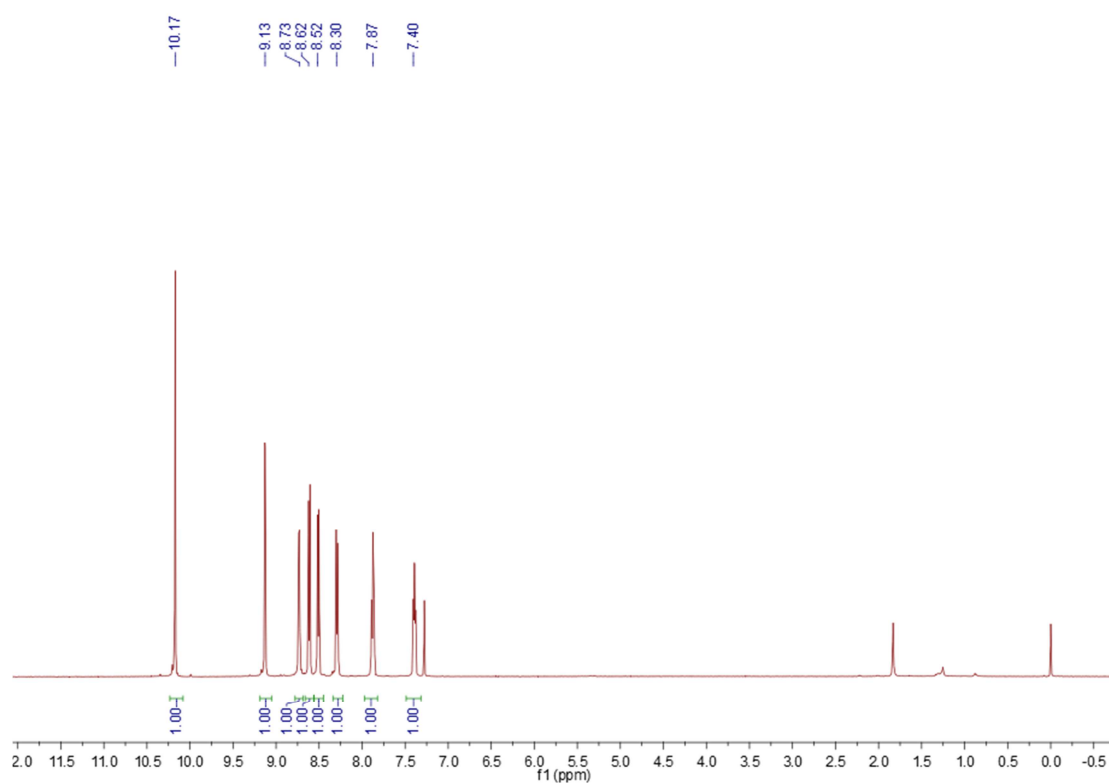


Fig.S1 The ^1H NMR of 5-aldehyde-2, 2'-bipyridine

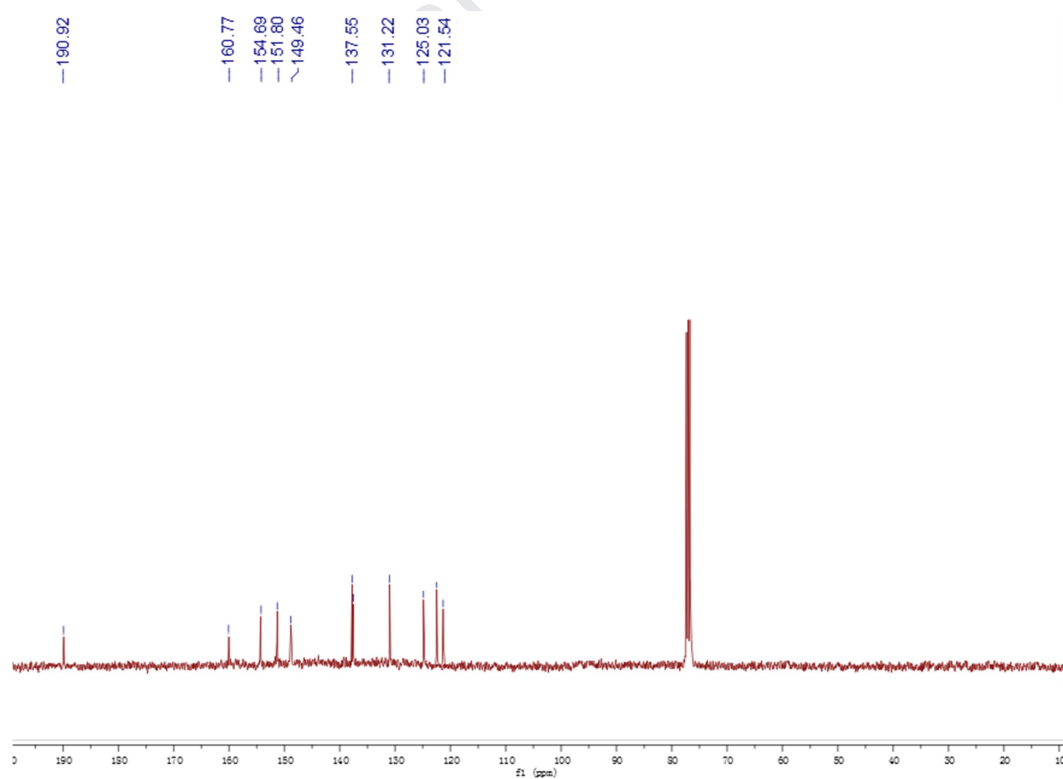


Fig.S2 The ^{13}C NMR of 5-aldehyde-2, 2'-bipyridine

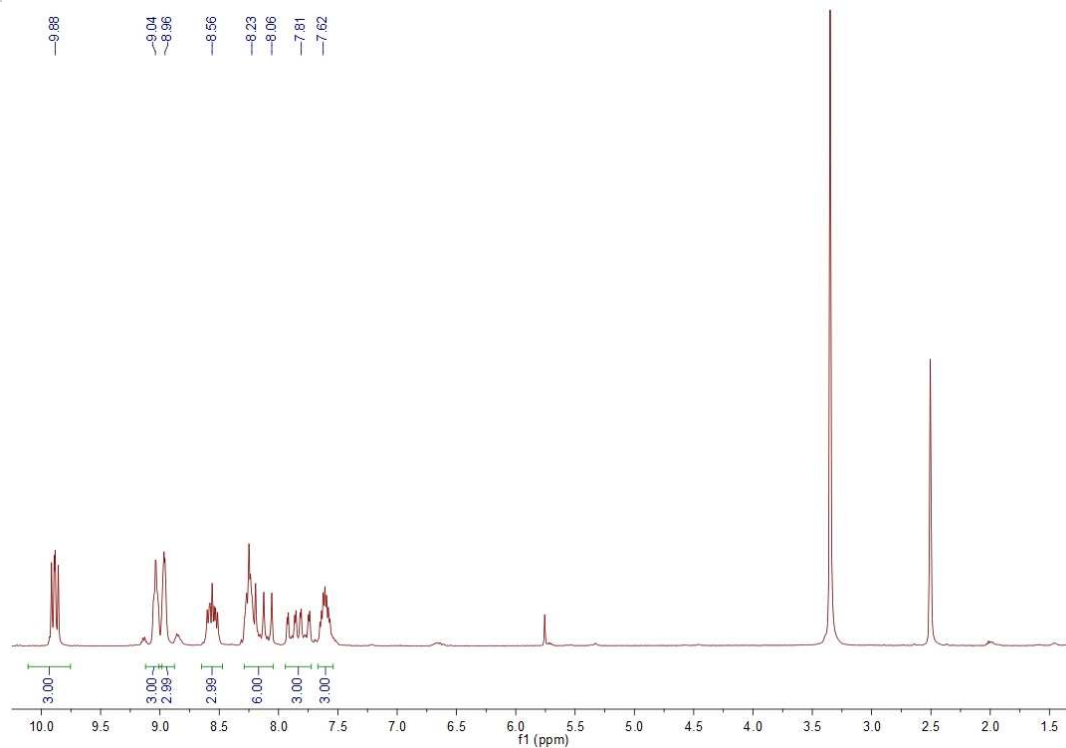


Fig.S3 The ^1H NMR of $[\text{Ru}(\text{CHO-bpy})_3]$ P1

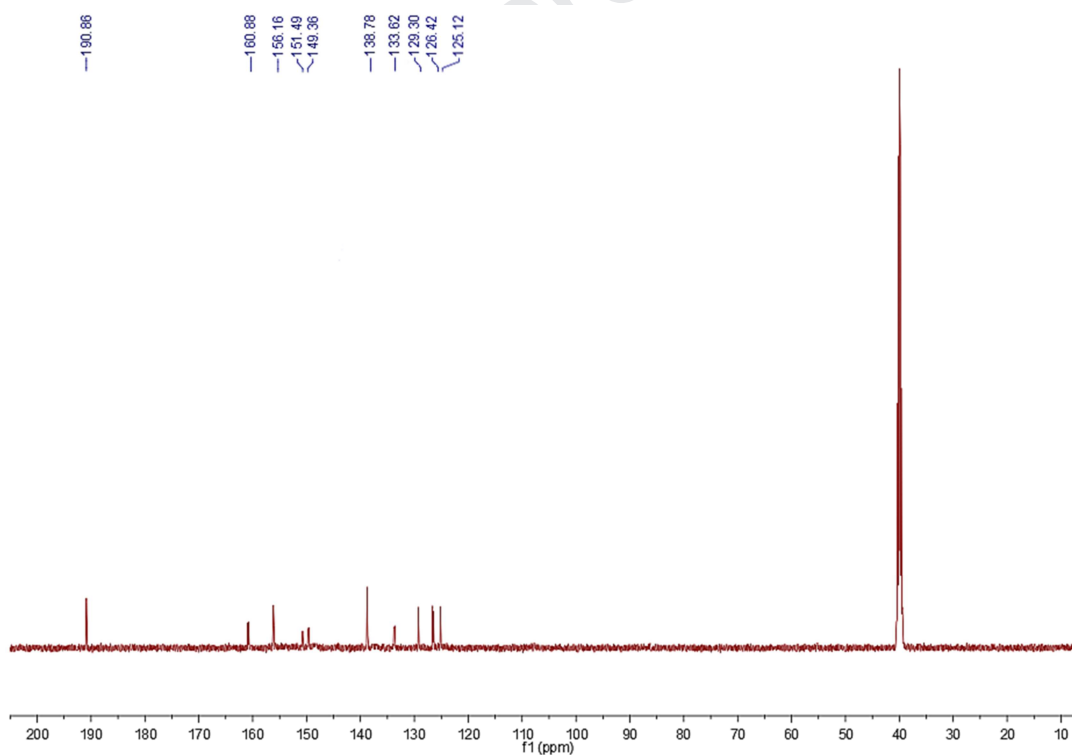


Fig.S4 The ^{13}C NMR of $[\text{Ru}(\text{CHO-bpy})_3]$ P1

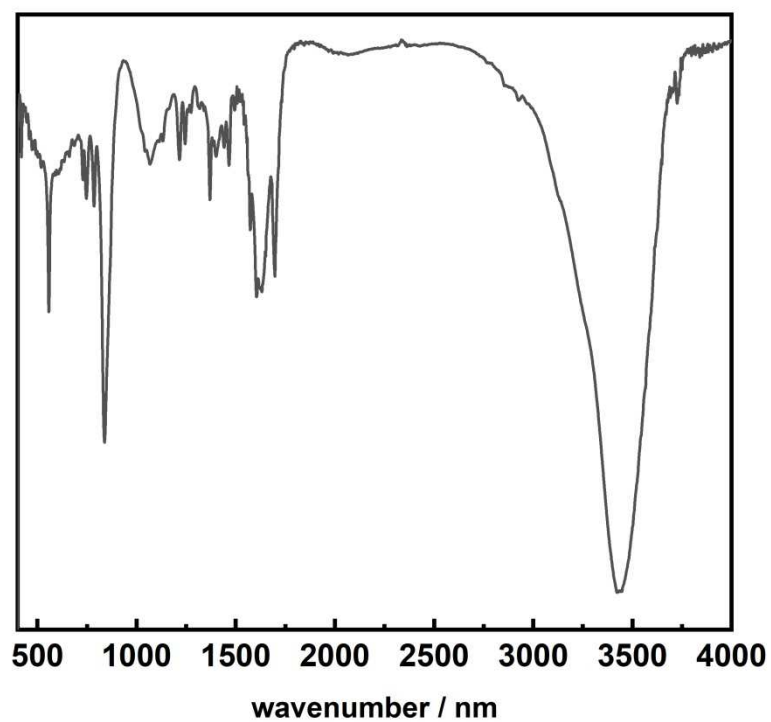


Fig.S5 The FT-IR of [Ru(CHO-bpy)₃]

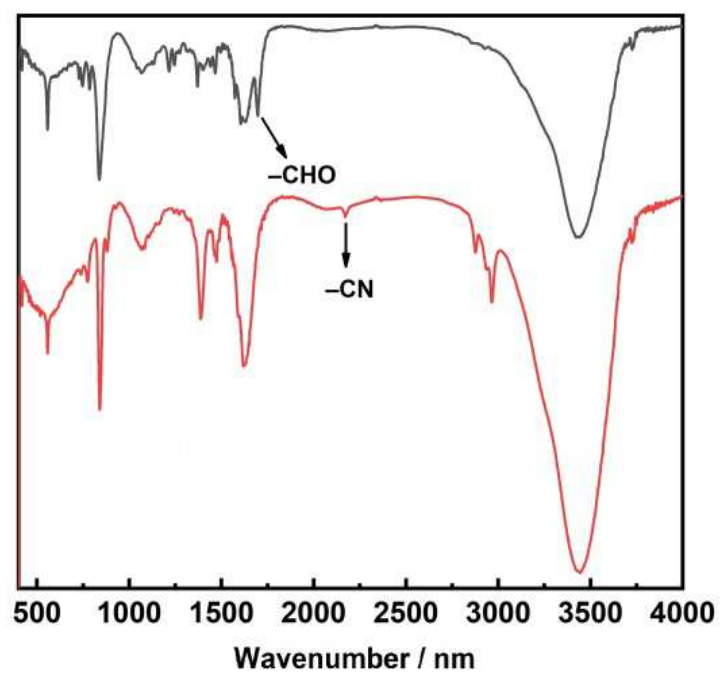
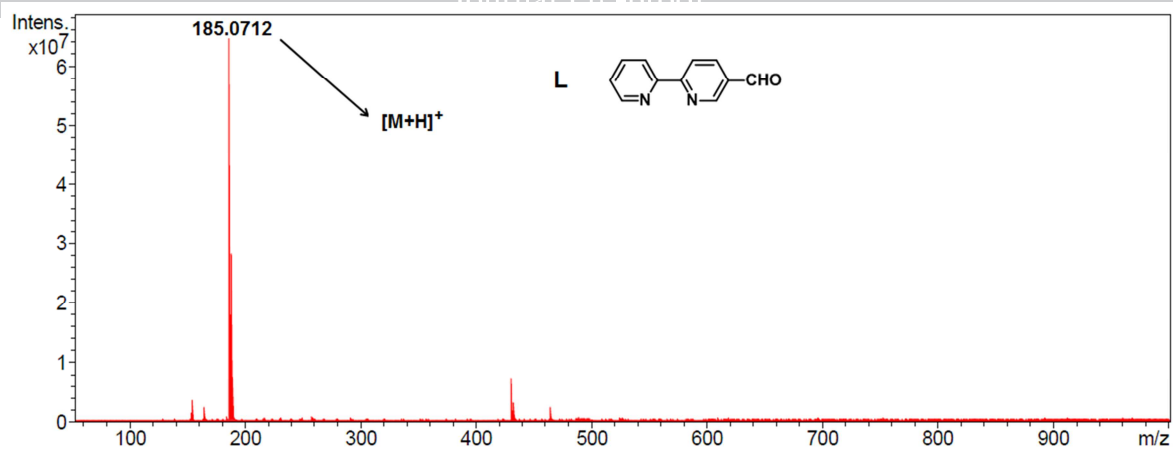
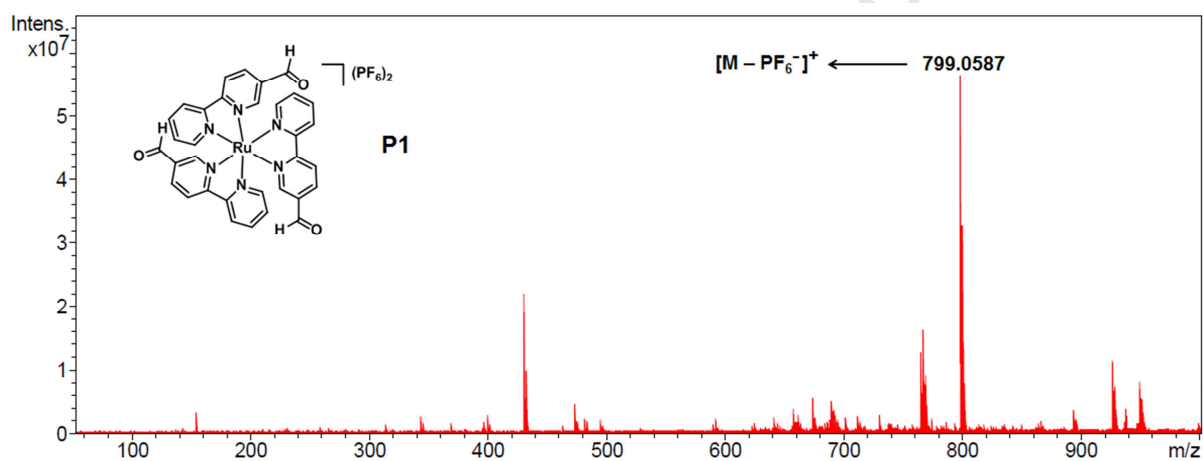
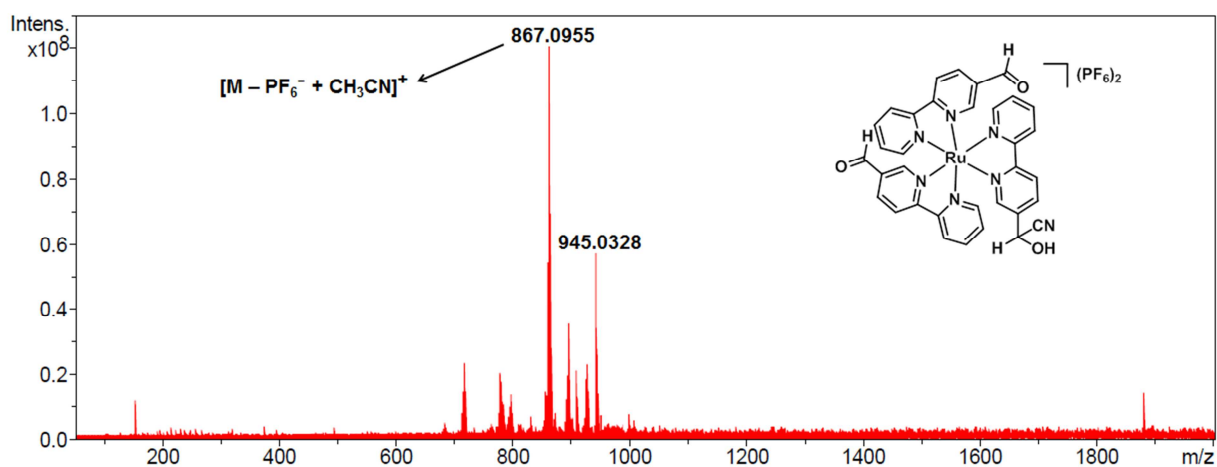


Fig.S6 FT-IR about P1 and P1 + 3CN⁻

**Fig.S7** HRMS spectrum of the ligand **L****Fig.S8** HRMS spectrum of the probe **P1****Fig.S9** HRMS spectrum of the **P1** + CN^- (1 : 1) in CH_3CN/H_2O (40/60, v/v)

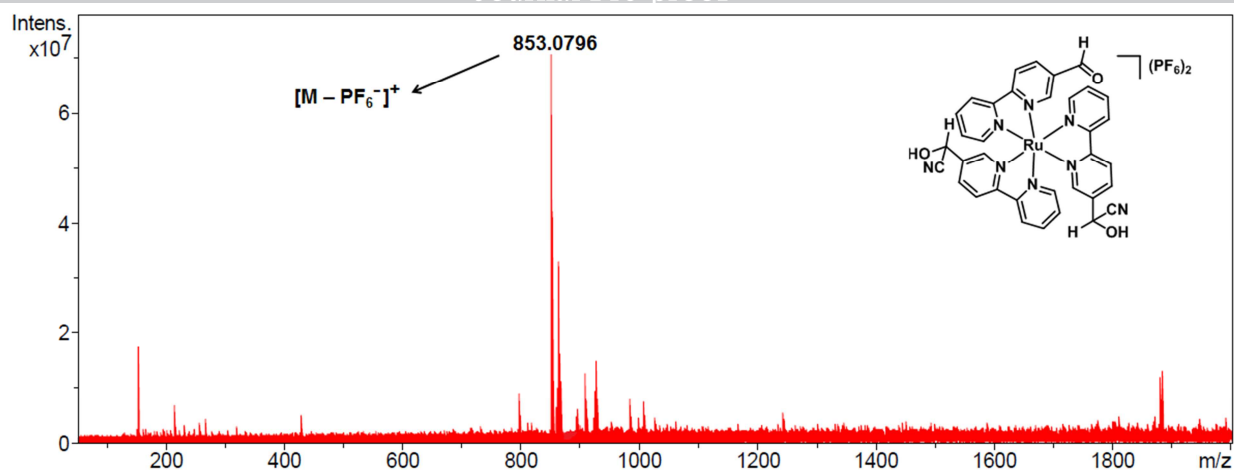


Fig.S10 HRMS spectrum of the **P1** + CN^- (1 : 2) in CH_3CN/H_2O (40/60, v/v)

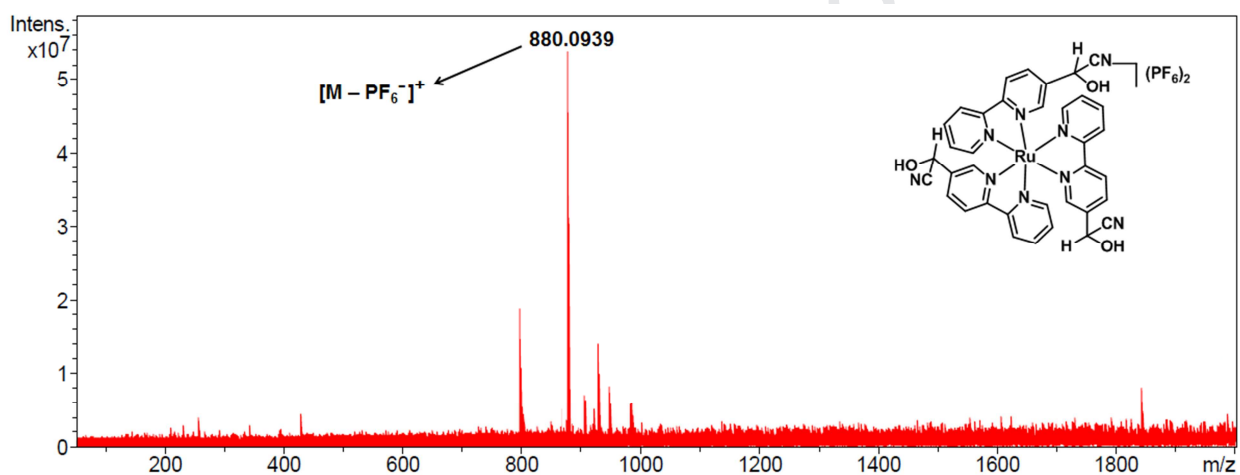


Fig.S11 HRMS spectrum of the **P1** + CN^- (1 : 3) in CH_3CN/H_2O (40/60, v/v)

Table S1. Crystallographic data and structure refinement parameters for **P1**

Compound	P1
Chemical formula	$C_{33}H_{24}F_{12}N_6O_3P_2Ru$
FW	943.59
T/[K]	173(2)
$\lambda/\text{\AA}$	1.34138
Crystal system	Triclinic
Space group	$P \bar{1}$
a/\AA	13.8556(7)
b/\AA	16.4412(8)
c/\AA	17.4777(8)
$\alpha/^\circ$	87.429(2)
$\beta/^\circ$	82.029(2)
$\gamma/^\circ$	84.196(2)
V/\AA^3	3920.9(3)
Z	4
$\rho/\text{Mg m}^{-3}$	1.598
μ/mm^{-1}	3.279
F(000)	1880
θ range/$^\circ$	2.815–55.997
Reflections collected	58831
Data/restraints/param	15490 / 106 / 1002
Goodness-of-fit on F^2	1.059
Final R indices [$I > 2\sigma(I)$]	R1 = 0.0740 wR2 = 0.2149
Largest diff. peak/hole ($e \text{\AA}^{-3}$)	2.237 and 1.334

^a $R1 = \sum ||F_o| - |F_c|| / \sum |F_o|$ (based on reflections with $F_o2 > 2\sigma F2$). $wR2 = [\sum [w(F_o2 - F_c2)^2] / \sum [w(F_o2)^2]]^{1/2}$; $w = 1/[\sigma^2(F_o2) + (0.095P)^2]$; $P = [\max(F_o2, 0) + 2F_c2]/3$ (also with $F_o2 > 2\sigma F2$).

Table S2. Crystal data and structure refinement for platon_sq.

Identification code	platon_sq	
Empirical formula	C33 H24 F12 N6 O3 P2 Ru	
Formula weight	943.59	
Temperature	173(2) K	
Wavelength	1.34138 Å	
Crystal system	Triclinic	
Space group	P $\bar{1}$	
Unit cell dimensions	a = 13.8556(7) Å	$\alpha = 87.429(2)^\circ$.
	b = 16.4412(8) Å	$\beta = 82.029(2)^\circ$.
	c = 17.4777(8) Å	$\gamma = 84.196(2)^\circ$.
Volume	3920.9(3) Å ³	
Z	4	
Density (calculated)	1.598 Mg/m ³	
Absorption coefficient	3.279 mm ⁻¹	
F(000)	1880	
Crystal size	0.200 x 0.080 x 0.060 mm ³	
Theta range for data collection	2.815 to 55.997°.	
Index ranges	-17 ≤ h ≤ 17, -20 ≤ k ≤ 20, -21 ≤ l ≤ 21	
Reflections collected	58831	
Independent reflections	15490 [R(int) = 0.0456]	
Completeness to theta = 53.594°	99.9 %	
Absorption correction	Semi-empirical from equivalents	
Max. and min. transmission	0.751 and 0.560	
Refinement method	Full-matrix least-squares on F ²	
Data / restraints / parameters	15490 / 106 / 1002	
Goodness-of-fit on F ²	1.059	
Final R indices [I > 2σ(I)]	R1 = 0.0740, wR2 = 0.2149	
R indices (all data)	R1 = 0.0772, wR2 = 0.2186	
Extinction coefficient	n/a	
Largest diff. peak and hole	2.237 and -1.334 e.Å ⁻³	

Highlights

- A stable and quick response ruthenium probe in aqueous solution (60 % water) with a detection limit of 0.75 μM was synthesized.
- The ruthenium complex showed good selectivity towards cyanide in a variety of anions and cations.
- A visual colorimetric strip based on the ruthenium complex showed good detection performance on CN^- ion with quick response time.

Declaration of interests

The authors declare that they have no known competing financial interests or personal relationships that could have appeared to influence the work reported in this paper.

The authors declare the following financial interests/personal relationships which may be considered as potential competing interests: